

# Generation of longitudinal flux tube waves in $\epsilon$ Eridani

Diaa E. Fawzy<sup>★</sup>

*Faculty of Engineering and Computer Sciences, Izmir University of Economics, 35330 Izmir, Turkey*

Accepted 2013 August 6. Received 2013 July 8; in original form 2013 June 5

## ABSTRACT

The aim of the current study is the computation of wave energy fluxes for longitudinal tube waves generated in the convection zone of the chromospherically active star  $\epsilon$  Eridani. In our models, we employ a modified theory of turbulence together with the magnetohydrodynamic equations in a time-dependent setting. The wave generation mechanism is given by the interaction between vertically oriented magnetic flux tubes and the convective turbulence. We also use updated values for the effective temperature and surface gravity; additionally, we take different magnetic activity levels into account. Our numerical approach allows for the non-linear effects to be considered. The time-averaged upward propagating energy fluxes range from  $F_{\text{LTW}} = 4.02 \times 10^7$  to  $2.92 \times 10^8$  ( $\text{erg cm}^{-2} \text{s}^{-1}$ ) for flux tubes of magnetic field strengths between  $B_0 = 1830 \text{ G}$  and  $1445 \text{ G}$ , respectively. This increase given as roughly a factor of 7 between the above mentioned values of the magnetic field strengths is attributable to the enhanced rigidity of the magnetic flux tube found for relatively large magnetic field strengths. The current results are highly significant for the construction of theoretical time-dependent model chromospheres.

**Key words:** MHD – methods: numerical – stars: chromospheres – stars: magnetic field.

## 1 INTRODUCTION

The magnetic field is considered constituting the driving entity for the majority of active phenomena observed on the Sun and other solar-type stars. Chromospheric and coronal activities are examples which reflect the role(s) of the magnetic field resulting in the observed spatial temperature increases beyond stellar photospheres (e.g. De Pontieu et al. 2011; McLaughlin, Hood & de Moortel 2011; Houdebine et al. 2012, and references therein). Stellar magnetic fields are highly complex in nature and there are no direct techniques to observe small-scale stellar magnetic field structure; therefore, we must rely on a theoretical approach to understand and interpret spectral lines correlated with stellar magnetic field features. This latter effort is highly challenging even for the Sun. Due to the lack of spatial resolution, solar-type magnetic features can in general not be observed on stars; in most cases, we are limited to a global view of magnetic surface fields; reviews on the subject of solar magnetic field and cool stars have been given by Solanki, Inhester & Schüssler (2006) and Reiners (2012). On the other hand, stars offer the opportunity of observing a wide range of magnetic field strengths and activities ultimately triggered by motions within the stellar convection zones, thus allowing us to enhance our understanding of magnetic dynamo theory.

The chromospheric temperature rise for the Sun and other solar-type stars is still a largely unsolved problem, but the two fundamental heating mechanisms, i.e. acoustic and magnetic, are widely accepted as they dominate in non-magnetic and magnetic regions, respectively (e.g. Klimchuk 2006; Taroyan & Erdélyi 2009; Morton et al. 2012; Wedemeyer-Böhm et al. 2012). Theoretical models based on these mechanisms can predict the radiative losses in chromospheric lines (e.g.  $\text{Mg II } h+k$  and  $\text{Ca II H+K}$ ) with acceptable accuracy; see, e.g. work by Ulmschneider (1989), Buchholz et al. (1998) and Cuntz, Rammacher & Musielak (2007) for acoustic waves, and, e.g. Fawzy et al. (2002a,b,c) for magnetic waves. Both mechanisms have previously been combined in two-component models to represent both the magnetic-free and magnetic regions (e.g. Cuntz, Ulmschneider & Musielak 1998; Cuntz et al. 1999); the realism of the time-averaged temperature rises beyond stellar photospheres in both acoustic and magnetic models has been assessed by, e.g. Rammacher & Cuntz (2005), among other work.

Various previous studies have been devoted to the dwarf star  $\epsilon$  Eridani as it is one of the closest late-type main-sequence stars known to almost certainly possessing a planet (Hatzes et al. 2000); it is also recognized for displaying high magnetic and chromospheric activity (e.g. Veytes, Mauas & Diaz 2009) due to its young age (e.g. Janson et al. 2008). In principle,  $\epsilon$  Eridani displays solar-like behaviour, despite pronounced differences in scales and magnitude. It has a higher global magnetic field than the Sun, noting that on average the magnetic field strength averaged over its surface is about  $165 \pm 30 \text{ G}$  (Rüedi et al. 1997). A study by Croll et al. (2006)

<sup>★</sup>E-mail: diaa.gadelmavla@ieu.edu.tr

confirms the earlier findings that the surface of  $\epsilon$  Eridani is rotating differentially analogous to the Sun. A magnetic activity cycle similar to the Sun has recently been confirmed by Metcalfe et al. (2013). Thus,  $\epsilon$  Eridani offers a unique opportunity for the study of stellar dynamos. Moreover,  $\epsilon$  Eridani's UV output, a direct consequence of its magnetic activity, is also relevant in the context of astrobiology noting that the strength of stellar UV emission may be related to the suitability of  $\epsilon$  Eridani's environment for extraterrestrial life (e.g. Cockell 1999; Buccino, Lemarchand & Mauas 2006; Guinan & Engle 2009; Cuntz et al. 2012).

Moreover,  $\epsilon$  Eridani is also a suitable candidate for the study of chromospheric oscillations. Previous studies for main-sequence stars were given by, e.g. Matthews et al. (2004), Bouchy et al. (2004), Stello et al. (2010), Chaplin et al. (2011a,b) and Huber et al. (2011). Numerous investigations show that stars with notable chromospheric activity exhibit atmospheric oscillations (e.g. Ulmschneider et al. 2001a), and that waves take the roles of heating the outer layers as well as of serving as a driving agent to trigger stellar oscillations. Hence, the oscillations occur as a natural response of the atmospheres regarding propagating acoustic and magnetic waves; these waves are also a good indicator of chromospheric activity as well. The levels of chromospheric activities and oscillations strongly depend on the generated magnetic and acoustic wave energies produced in the stellar convection zones. Chromospheric activity and the stellar oscillation frequencies are closely related to the stellar effective temperature as well as to the surface gravity; in particular the oscillation frequencies increase with decreasing the effective temperature regarding main-sequence stars.

The current work is an extension and application of the previous work by Ulmschneider, Musielak & Fawzy (2001b) in which the main mechanism responsible for the generation of different types of waves (i.e. longitudinal and transverse) was identified as the perturbation of the magnetic flux bundles (magnetic flux tubes) by turbulence in the stellar convection zones. Note that there is no comprehensive approach to the treatment of the various types of waves relevant to the heating of stellar chromospheres and coronae; typically, they require noticeably different algebraic and numerical methods. In the present study, we focus on the calculation of the energy generated by longitudinal waves (LTWs). Our aim is to compute the amount of magnetic wave energy fluxes for  $\epsilon$  Eridani while considering updated stellar parameters; this will furthermore prevent the appearance of numerical errors expected to occur when interpolating results from general studies. Obtaining the required values constitutes step 1 towards constructing self-consistent and time-dependent magnetic chromospheric models.

In summary, the determination of the energy fluxes in form of LTWs is of great significance to the following future efforts. (1) Energy input studies for outer stellar layers taking  $\epsilon$  Eridani as an example; it also includes the opportunity of assessing possible star–planet interactions in the view of recent studies on Ca II emission enhancement in planet-hosting stars (e.g. Krejčová & Budaj 2012, and references therein). (2) Astrobiological studies considering that stellar UV radiation is correlated to the underlying magnetic energy budget, which appears to be relevant in the context of extraterrestrial life (e.g. Cockell 1999; Guinan & Engle 2009). (3) Atmospheric oscillation studies in consideration of that stellar atmospheres strongly react to propagating waves (e.g. Kalkofen et al. 1994; Fawzy & Musielak 2012, and references therein).

This paper is structured as follows: a description of the methodology of computation is given in Section 2, Section 3 presents the results and discussion, whereas the conclusions are given in Section 4.

---

**Algorithm 1: Main**


---

**input** :  $T_{eff}$ : Effective temperature;  $\mathcal{G}$ : Surface gravity;  $Z_m$ : Metallicity;  $\mathcal{B}$ : Magnetic field strength;  $\alpha$ : Mixing length parameter  
**output**:  $UPW$ : Upward propagating wave spectra;  $\mathcal{E}$ : Time-averaged energy flux.

```

1 begin
2    $\langle \mathcal{M}, \mathcal{U}_t, \mathcal{V}_\parallel \rangle \leftarrow InitialModels(T_{eff}, \mathcal{G}, Z_m, \mathcal{B}, \alpha)$ ;
3    $\langle UPW, \mathcal{E} \rangle \leftarrow ComputeInteractions(\mathcal{M}, \mathcal{U}_t, \mathcal{V}_\parallel)$ ;
4   return  $\langle UPW, \mathcal{E} \rangle$ 
5 end
```

---



---

**Algorithm 2: Initial Models**


---

**input** :  $T_{eff}$ : Effective temperature;  $\mathcal{G}$ : Surface gravity;  $Z_m$ : Metallicity;  $\mathcal{B}$ : Magnetic field strength;  $\alpha$ : Mixing length parameter  
**output**:  $\mathcal{M}$ : Magnetic flux tube;  $\mathcal{U}_t$ : Convection zone;  $\mathcal{V}_\parallel$ : Turbulence.

```

1 begin
2    $\mathcal{M} \leftarrow generate\_mft(T_{eff}, \mathcal{G}, Z_m, \mathcal{B})$ ;
3    $\mathcal{U}_t \leftarrow generate\_convection(T_{eff}, \mathcal{G}, Z_m, \alpha)$ ;
4    $\mathcal{V}_\parallel \leftarrow generate\_turbulence(\mathcal{U}_t)$ ;
5   return  $\langle \mathcal{M}, \mathcal{U}_t, \mathcal{V}_\parallel \rangle$ 
6 end
```

---



---

**Algorithm 3: ComputeInteractions**


---

**input** :  $\mathcal{M}$ : Magnetic flux tube;  $\mathcal{V}_\parallel$ : Turbulence;  $\beta$ : integer.  
**output**:  $UPW$ : Upward propagating wave spectra;  $\mathcal{E}$ : time-averaged energy flux.

```

1 begin
2    $t \leftarrow t_{initial}$ ;
3    $\mathcal{W} \leftarrow empty$ ;
4    $\mathcal{E} \leftarrow empty$ ;
5   while  $t \leq \beta$  do
6      $\mathcal{W}^t \leftarrow mhd(t, \mathcal{M}, \mathcal{V}_\parallel)$ ;
7      $\mathcal{E}^t \leftarrow avg\_energy\_flux(\mathcal{W}^t)$ ;
8     increment  $t$ ;
9    $\mathcal{W} \leftarrow interpolate(\mathcal{W})$ ;
10   $\mathcal{W}'' \leftarrow apodize(\mathcal{W})$ ;
11   $\mathcal{P} \leftarrow fft(\mathcal{W}'')$ ;
12   $\mathcal{PW} \leftarrow high\_pass\_filter(\mathcal{P})$ ;
13   $UPW \leftarrow fft^{-1}(\mathcal{PW})$ ;
14  return  $\langle UPW, \mathcal{E} \rangle$ 
15 end
```

---

**Figure 1.** The algorithm used for the current computations.

## 2 METHODOLOGY OF MAGNETIC FLUX-TUBE ENERGY GENERATION

The algorithms shown in Fig. 1 summarize the procedure used in the current computations, and the following subsections explain the computational steps in detail.

### 2.1 Initial model parameters

There are essentially four parameters which uniquely specify a star, which are: the effective temperature  $T_{eff}$ , surface gravity  $g$ , metallicity  $Z_m$  and rotation period. The latter is an important parameter for the computation of the magnetic wave energy flux at the stellar surface since the dynamics within the stellar convective zone is critically affected by rotation. The stellar rotation is directly correlated with the magnetic filling factor (e.g. Cuntz et al. 1999, and references therein); however, in the current computations we employ our procedure to a specific flux-tube model associated with a fixed stellar surface magnetic filling factor. As part of our models we also consider the effects of metal abundances on the efficiency of acoustic and magnetic wave generation. Relevant previous investigations concern both analytical works, given by Ulmschneider et al. (1999) for acoustic waves and Musielak, Rosner & Ulmschneider (2002) for magnetic waves.

In the view of recent studies, the basic stellar parameters for  $\epsilon$  Eridani, namely, the effective temperature  $T_{eff}$ , the surface gravity

**Table 1.** Basic parameters for atmospheric models of  $\epsilon$  Eridani.

$T_{\text{eff}}$ (K)	$\log g$ –	$B_{\text{eq}}$ (G)	$r_b$ (km)	$M/M_{\odot}$ –	[Fe/H] –
5084	4.30	1926	50.0	0.82	−0.13

$\log g$  and the metallicity are now largely settled, albeit small uncertainties remain. The updated values are given as  $T_{\text{eff}} = 5084 \pm 5.9$  K (Kovtyukh et al. 2003),  $\log g = 4.30 \pm 0.08$  (Gonzalez, Carlson & Tobin 2010) and metallicity [Fe/H] =  $-0.13 \pm 0.04$  (Santos, Israelian & Mayor 2004). These values are summarized in Table 1; they form the basis for the current computations. The opacity tables computed by the ATLAS code of Kurucz (1992, 1996) are used in our study.

## 2.2 Magnetic flux-tube models

In the current study, we use the widely accepted concept of the thin flux-tube approximation (e.g. Stenflo 1978; Solanki 1993) as guidance; note that this concept has been validated through numerous computations once the flux-tube extension with height does not exceed few pressure scale-heights (Hassan et al. 2003); this assumption is readily fulfilled in the current computations. Thus, we consider a vertically oriented thin magnetic flux tube embedded in a field-free region at height  $z = 0$  km.

The construction of the initial flux-tube models requires the determination of the magnetic field strength at the base of the flux tube (height  $z = 0$  km). Because of the lack of spatial resolution on stellar surfaces, the parameters of stellar magnetic features (field strength,  $B_0$  and the magnetic filling factor,  $f_0$ ) cannot accurately be determined, and the factors of  $B_0/f_0$  cannot easily be separated. The magnetic flux tubes are bundles of field lines governed by the horizontal pressure balance with their surroundings, which also defines the upper limit of the magnetic field strength inside of the tubes. The maximum value is reached in the limiting case of void tubes (i.e. internal gas pressure  $p_i = 0$ ); this case corresponds to the equipartition field strength,  $B_{\text{eq}}$ ; it is obtained from the horizontal pressure balance equation  $B_{\text{eq}}^2/8\pi + p_i = p_e$  with  $p_e$  being the external gas pressures at the same height. For most GK-type stars, Saar (1996) found that the magnetic field strength  $B \leq B_{\text{eq}}$  is commonly valid, although heavily spotted stars may violate this approach; however, these types of stars are beyond the scope of our study.

In the current models, we obtain a value of  $p_e(z = 0 \text{ km}) = 1.48 \times 10^5 \text{ dyn cm}^{-2}$  corresponding to  $B_{\text{eq}} = 1926$  G. To determine the bottom radius of the flux tube, we consider the solar case as guidance. Note that on the Sun, a thin magnetic flux tube has a radius of roughly half the local pressure scaleheight,  $r_b \simeq \Re T_{\text{eff}}/2\mu g$ , where  $\mu$  is the mean molecular weight and  $\Re$  is the gas constant. For  $\epsilon$  Eridani, a tube radius  $r_b = 50$  km is attained. As the magnetic field strength changes across the stellar surface, we assume a set of three different factors,  $\eta = B/B_{\text{eq}} = 0.75, 0.85$  and  $0.95$ . For the Sun, a value of  $B/B_{\text{eq}} = 0.875$  is implied based on an equipartition field of  $B_{\text{eq}} = 1715$  G. The choice of these factors is supported by a study of Valenti, Marcy & Basri (1995), which indicates that 9 per cent of the star's surface is covered by 1.44 kG field, corresponding to about  $0.75 B_{\text{eq}}$  in the current computations.

With the specification of the parameters stellar effective temperature, surface gravity and the magnetic field strength at height  $z = 0$  km we construct a vertically oriented magnetic flux-tube model embedded in a field-free region as shown in step 2 of the main algorithm (see Fig. 1). An intriguing aspect is the height

where the interaction between the magnetic flux tubes and the turbulent eddies takes place. The interaction is expected to be near the stellar surface where the maximum turbulent velocities occur. A previous study by Ulmschneider & Musielak (1998) indicates that the position of the squeezing point has no significant influence on the properties of the generated magnetic waves. Hence, we assume as height of the squeezing point  $\tau_{5000} = 1$  consistent with the aforementioned study; it also indicates that the magnetic filling factor and the flux-tube geometry do not need to be taken into account in the context of magnetic energy generation simulations.

## 2.3 Convection zone model

In the following, we adopt the paradigm that the intercorrelation between the stellar convective zone, differential rotation and the magnetic field is key for modelling stellar chromospheric and coronal activity. As the depth of the convective zone increases with decreasing stellar effective temperature, the K2 star  $\epsilon$  Eridani is identified as convectively active, possessing chromospheric activity similar to the Sun, albeit significantly larger in magnitude (Sim & Jordan 2005). The construction of convection zone models within the current study is based on the mixing-length theory described by Theurer (1993), which is supported by 3D simulations for the Sun attained by Stein et al. (2009a,b). They found that a mixing-length parameter of  $\alpha = 1.8$  matches well with the classical mixing-length computations. In the context of our models, we perform computations for a set of different values of  $\alpha = 1.6, 1.8$  and  $2.0$ . Step 4 of the second algorithm (see Fig. 1) generates a convection zone model for a given set of parameters ( $T_{\text{eff}}, \log g, Z_m$  and  $\alpha$ ).

## 2.4 Magnetic flux tube–turbulence interaction

Contrary to the analytical approach, the current treatment allows for the generation of non-linear waves with large amplitudes. The algorithms shown in Fig. 1 summarize the numerical approach followed in the current study; for more details refer to the original development by Ulmschneider & Musielak (1998) and the subsequent modifications by Ulmschneider et al. (2001b).

We simulate the interaction between a vertically oriented magnetic flux tube (step 2 of the second algorithm) and the convective turbulence (step 4 of the second algorithm) as a deriving mechanism for wave generations. The external pressure fluctuations generated by convective turbulence are responsible for squeezing the flux tubes and are represented by a superposition of  $N = 500$  partial sinusoidal waves. This number is considered sufficient for covering the whole range of the spectrum. The amplitudes of the partial waves are determined from the extended Kolmogorov spatial turbulent energy spectrum and the modified Gaussian frequency factor as described by Musielak et al. (1994). The current approach is based on determining the value of the rms turbulent velocity fluctuations,  $u_t$  near the stellar surface (overshooting region) where the squeezing of the flux takes place. As the maximum turbulent velocity on stars cannot be determined observationally, we rely on theoretical models. Solar observations and theoretical simulations confirm that the rms turbulent velocity at the overshooting region is about half the maximum turbulent velocity (Steffen 1993; Ulmschneider et al. 2001b). We keep the same factor for the current computations. The obtained maximum turbulent velocities for the dwarf star  $\epsilon$  Eridani are  $u_{\text{max}} = 2.03, 2.14$  and  $2.22 \text{ km s}^{-1}$  for  $\alpha = 1.5, 1.8$  and  $2.0$  respectively.

The calculated velocities define the pressure fluctuations that squeeze the flux tube. According to the pressure balance equation,

the gas perturbations outside the tube can be translated into internal longitudinal velocity fluctuations  $v_{\parallel}$  specified at the squeezing height. It also serves as a bottom boundary condition in the MHD wave code. As the computations of the generated longitudinal flux by Ulmschneider & Musielak (1998) show little dependence on the location of the squeezing, the squeezing point of the tube in the current computations is chosen at  $z = 0$  km corresponding to the optical depth  $\tau_{5000} = 1$ . With the specification of  $v_{\parallel}(z = 0, t)$ , the instantaneous values of the internal pressure perturbation  $p'(z = 0, t)$  can be computed by utilizing a modified version of a time-dependent, magnetohydrodynamic Lagrangian code (Herbold et al. 1985). The interactions are followed in time; the time sequence of the instantaneous wave energy fluxes,  $F(z, t) = v_{\parallel}(z, t)p'(z, t)$ , and the time-averaged wave energy flux,  $\overline{F}(z, t)$  at the squeezing height are also computed. These steps are described in steps 2–8 of the third algorithm shown in Fig. 1.

In our computations of the energy fluxes and spectra of the upward propagating longitudinal flux-tube waves, we first perform a forward Fourier transform to obtain instantaneous wave energy fluxes and velocities; thereafter, we apply a high pass filter at the Defouw cutoff frequency to filter out the propagating waves. This step is followed by an inverse Fourier transform to convert back the propagating waves into time domain and then calculating both the time-averaged energy flux and spectra (see steps 9–14 of the third algorithm; see Fig. 1). The current computations are done adiabatically and the height of the flux tube is limited to a small domain only to avoid (sub)photospheric shock formation.

### 3 RESULTS

#### 3.1 Magnetic wave energy fluxes

The generated waves depict a wide range of frequencies and a mixture of propagating and non-propagating components. This type of classification is based on the Defouw cutoff frequency  $\omega_D$  (Defouw 1976); waves with frequencies  $\omega > \omega_D$  are called propagating and called non-propagating otherwise. As we are interested in the contribution of upward propagating waves, we employ Fourier analysis techniques to convert the time sequence of the velocity and pressure perturbations into the frequency domain and then set up a high pass filter at the Defouw cutoff frequency to separate propagating and non-propagating waves. The generated fluxes are very spiky as depicted in Fig. 2. For the computation of meaningful time-averaged energy fluxes we thus run our computations for about  $\beta = 35P_D$  with  $P_D$  denoting the wave period corresponding to the Defouw cutoff frequency (Defouw 1976). For  $\epsilon$  Eridani,  $\omega_D$  is given as 0.0035 Hz; note that only upward propagating waves are computed.

Observations of the Sun show that the magnetic field strength at the base of the flux tube is of the order of  $B_0 = 1500$  G, which corresponds to a ratio  $B/B_{\text{eq}} = 0.875$ . The same ratio yields a value of  $B_0 = 1685$  G for  $\epsilon$  Eridani; furthermore, the rms turbulent velocity at the overshooting region in the  $\epsilon$  Eridani model is of the order of  $u_t = 1.1 \text{ km s}^{-1}$  compared to  $u_t = 1.3 \text{ km s}^{-1}$  for the Sun. The decrease in the obtained energy flux for  $\epsilon$  Eridani by roughly a factor of 2 compared to the Sun ( $F_{\text{LTW}} = 2.80 \times 10^8 \text{ erg cm}^{-2} \text{ s}^{-1}$ ; Fawzy, Cuntz & Rammacher 2012) is attributable to the decrease in the rms turbulent velocity. The difference in the obtained fluxes for  $\epsilon$  Eridani is mainly due to the differences in the magnetic field strengths, whereas the different rms turbulent velocities are only of minor importance.

Table 2 summarizes the obtained results for different magnetic field strengths and mixing-length parameters. The obtained results

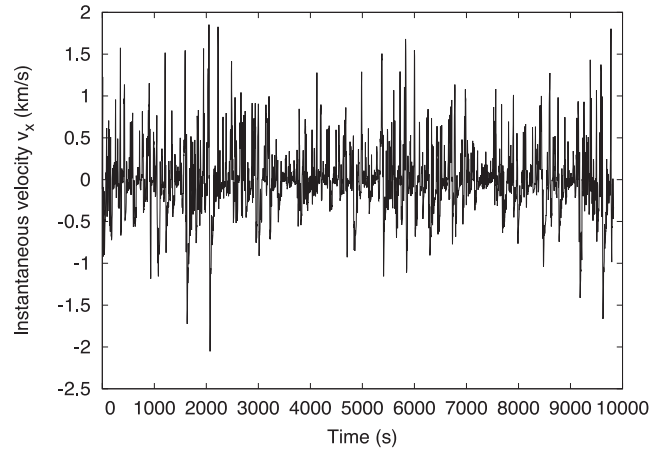


**Figure 2.** Instantaneous velocity fluctuations outside of magnetic flux tubes at height  $z = 0$  km for models of  $\epsilon$  Eridani with  $\eta = 0.85$  and mixing-length parameter  $\alpha = 1.8$ .

**Table 2.** The rms turbulent velocity  $u_t$  ( $\text{cm s}^{-1}$ ), acoustic  $F_{\text{ac}}$  and magnetic wave energy flux  $F_{\text{LTW}}$  ( $\text{erg cm}^{-2} \text{ s}^{-1}$ ) for different parameters of  $\alpha$  and  $\eta$ .

$\alpha$	$u_t$	$F_{\text{ac}}$	$\eta = 0.75$	$\eta = 0.85$	$\eta = 0.95$
1.5	1.00E5	1.73E7	1.95E8	1.27E8	4.02E7
1.8	1.07E5	3.22E7	2.36E8	1.46E8	4.33E7
2.0	1.11E5	4.62E7	2.92E8	1.74E8	5.17E7

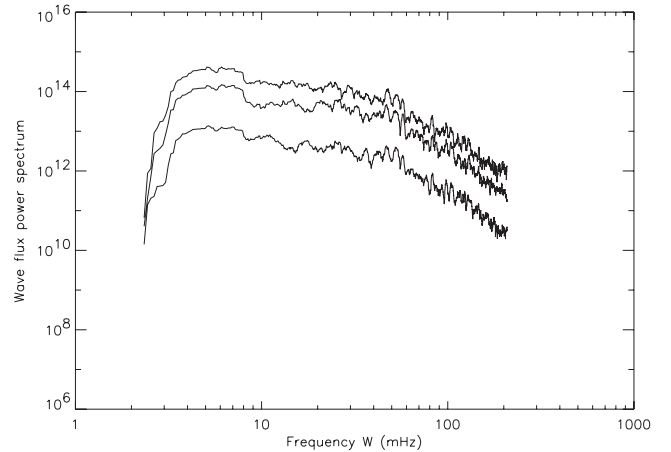


**Figure 3.** Wave flux power spectrum for upward propagating waves for models of  $\epsilon$  Eridani with  $\eta = 0.75$  (highest), 0.85 and 0.95 (lowest) and mixing-length parameter  $\alpha = 1.8$ .

show a strong dependence of the generated fluxes on the value of the mixing-length parameter  $\alpha$ ; note that the fluxes increase roughly by a factor of 1.4 for an increase of  $\alpha$  by a value of 0.5. Based on state-of-the-art simulations by Stein et al. (2009a,b), the best choice for  $\alpha$  given as  $\alpha = 1.8$  implies that the flux decreases by a factor of 5.5 from  $\eta = 0.75$  to 0.95. This behaviour is due to the fact that the efficiency of longitudinal tube waves generation decreases with the stiffness of magnetic flux tubes, which are relatively resistant to squeezing by external turbulence. The obtained spectra extend over about 200 mHz and reach their maximum values at about  $\omega_{\text{max}} = 2.0\omega_D$  as shown in Fig. 3. The obtained fluxes indicate that



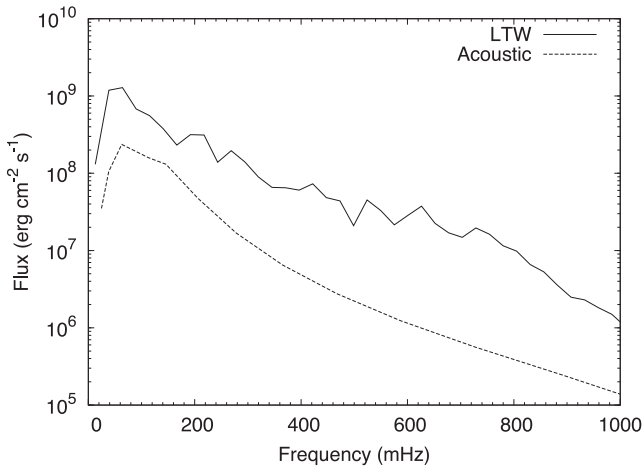


**Figure 4.** A comparison between the generated flux for acoustic and magnetic waves, i.e.  $F_{ac}$  (dashed) and  $F_{LTW}$  (solid), for models of  $\epsilon$  Eridani with  $\eta = 0.85$  and mixing-length parameter  $\alpha = 1.8$ .

the chromospheric activity of  $\epsilon$  Eridani may at least partially be attributable to the dissipation of LTWs akin to the Sun.

### 3.2 Comparison to the acoustic energy flux

In addition to the energy carried by LTWs along magnetic flux tubes, there is also a significant amount of acoustic energy produced by turbulent motions in the non-magnetic regions surrounding the magnetic flux tubes. It would be interesting to compare the computed LTW energy fluxes and spectra to those carried by acoustic waves outside the magnetic flux tubes. To compute the resulting acoustic wave energy spectra and fluxes, we employ the method described by Ulmschneider, Theurer & Musielak (1996) and use the same values of the input parameters, namely, the effective temperature  $T_{eff}$ , gravity  $\log g$  and the metallicity  $Z_m$  as given in Table 1; for the mixing-length parameter, we take  $\alpha = 1.8$ .

The obtained acoustic wave energy flux shows a decrease by a factor of about 4.5 compared to the magnetic wave energy flux using the same stellar parameters. Furthermore, both the acoustic and magnetic wave energy spectra show a rapid decrease at higher frequencies by roughly a factor of  $10^3$  over a frequency interval of 1000 mHz. A comparison between both spectra is depicted in Fig. 4. The obtained fluxes (i.e. acoustic and magnetic) can be combined to construct two-component stellar chromosphere models. Previous results have been obtained by Cuntz et al. (1999) and Fawzy et al. (2012) for the Sun and other solar-type stars for a broad range of magnetic activities.

## 4 CONCLUSIONS

In our current study, we focus on the computation of wave energy fluxes for longitudinal tube waves pertaining to the chromospherically active star  $\epsilon$  Eridani. This work is motivated through the general interest in outer atmospheric studies of solar-type stars both encompassing stellar heating processes and the generation of atmospheric oscillations. Additionally,  $\epsilon$  Eridani is an interesting object in the context of astrobiology considering that stellar UV radiation appears to be relevant in exobiological environments (e.g. Horneck 1995; Cockell 2002).

Thus, we computed the LTW energy spectra and fluxes resulting from the interaction between a vertically oriented magnetic flux tube

and turbulent motions in the stellar convection zone. The presented results are a first step towards developing time-dependent models for the chromosphere of  $\epsilon$  Eridani based on realistically generated wave energy and spectra. We use the updated values for the effective temperature, gravity, as well as the mixing-length parameter  $\alpha = 1.8$ . The following points summarize the obtained results.

(i) The obtained wave energy spectrum and flux carried by LTWs along magnetic flux tubes show similar trends as identified for the Sun; particularly, the spectrum reaches its maximum value at about  $\omega_{max} = 2.0\omega_D$  and decreases at higher frequencies.

(ii) The value of the magnetic field strength at the base of the flux tube has a significant influence on the obtained spectrum and flux. For a fixed value of  $\alpha = 1.8$ , the flux decreases by a factor of 5.5 from  $\eta = 0.75$  to 0.95. This is due to the fact that increasing the magnetic field pressure inside flux tubes enhances the stiffness of the tubes, which makes it difficult for the external turbulence squeezing the tube.

(iii) A maximum time-averaged upward propagating magnetic energy flux of  $F_{LTW} = 2.92 \times 10^8 \text{ erg cm}^{-2} \text{ s}^{-1}$  is obtained for magnetic flux tube with  $\eta = 0.75$  and  $\alpha = 2.0$ .

(iv) The obtained magnetic flux is sensitive to the value of the mixing-length parameter  $\alpha$ . The flux increases for increasing  $\alpha$ ; note that an increase by a factor of 1.4 is obtained when  $\alpha$  increases from 1.5 to 2.0.

We note that the obtained results are for individual magnetic flux tubes only. Furthermore, the magnetic filling factor within  $\epsilon$  Eridani's photosphere is not considered as part of the current computations. However, the presented results indicate that the generated magnetic energy flux is relevant for heating the outer atmospheric layers of this star. The obtained results will allow the construction of self-consistent and time-dependent model chromosphere for  $\epsilon$  Eridani in the context of future work.

## ACKNOWLEDGEMENTS

The author is grateful to an anonymous referee for detailed comments and for several important suggestions that allowed to significantly improve the paper. This work has been supported by the Faculty of Engineering and Computer Sciences, Izmir University of Economics. The author would also like to thank Z. E. Musielak and M. Cuntz for their valuable comments on an earlier version of the manuscript.

## REFERENCES

- Bouchy F., Maeder A., Mayor M., Megevand D., Pepe F., Sosnowska D., 2004, *Nat*, 432, 2
- Buccino A. P., Lemarchand G. A., Mauas P. J. D., 2006, *Icarus*, 183, 491
- Buchholz B., Ulmschneider P., Cuntz M., 1998, *ApJ*, 494, 700
- Chaplin W. J. et al., 2011a, *ApJ*, 732, L5
- Chaplin W. J. et al., 2011b, *ApJ*, 732, 54
- Cockell C. S., 1999, *Icarus*, 141, 399
- Cockell C. S., 2002, in Horneck G., Baumstark-Khan C., eds, *Astrobiology: The Quest for the Conditions of Life*. Springer, Berlin, p. 219
- Croll B. et al., 2006, *ApJ*, 648, 607
- Cuntz M., Ulmschneider P., Musielak Z. E., 1998, *ApJ*, 493, L117
- Cuntz M., Rammacher W., Ulmschneider P., Musielak Z. E., Saar S. H., 1999, *ApJ*, 522, 1053
- Cuntz M., Rammacher W., Musielak Z. E., 2007, *ApJ*, 657, L57
- Cuntz M., von Bloh W., Schröder K.-P., Bounama C., Franck S., 2012, *Int. Journal of Astrobiology*, 11, 15
- De Pontieu B. et al., 2011, *Sci*, 331, 55

- Defouw R. J., 1976, *ApJ*, 209, 266
- Fawzy D. E., Musielak Z. E., 2012, *MNRAS*, 421, 159
- Fawzy D., Rammacher W., Ulmschneider P., Musielak Z. E., Stępień K., 2002a, *A&A*, 386, 971
- Fawzy D., Ulmschneider P., Stępień K., Musielak Z. E., Rammacher W., 2002b, *A&A*, 386, 983
- Fawzy D., Stępień K., Ulmschneider P., Rammacher W., Musielak Z. E., 2002c, *A&A*, 386, 994
- Fawzy D. E., Cuntz M., Rammacher W., 2012, *MNRAS*, 426, 1916
- Gonzalez G., Carlson M. K., Tobin R. W., 2010, *MNRAS*, 403, 1368
- Guinan E. F., Engle S. G., 2009, in Griffin R. E., Hanisch R. J., Seaman R. L., eds, *Proc. IAU Symp. 258, The Ages of Stars*. Cambridge Univ. Press, Cambridge, p. 395
- Hassan S. S., Kalkofen W., van Ballegooijen A. A., Ulmschneider P., 2003, *ApJ*, 585, 1138
- Hatzes A. P. et al., 2000, *ApJ*, 544, L145
- Herbold G., Ulmschneider P., Spruit H. C., Rosner R., 1985, *A&A*, 145, 157
- Horneck G., 1995, *J. Photochem. Photobiol. B: Biology*, 31, 43
- Houdebine E. R., Butler C. J., Garcia-Alvarez D., Telting J., 2012, *MNRAS*, 426, 1591
- Huber D. et al., 2011, *ApJ*, 743, 143
- Janson M., Reffert S., Brandner W., Henning T., Lenzen R., Hippler S., 2008, *ApJ*, 488, 771
- Kalkofen W., Rossi P., Bodo G., Massaglia S., 1994, *A&A*, 284, 976
- Klimchuk J. A., 2006, *Sol. Phys.*, 234, 41
- Kovtyukh V. V., Soubiran C., Belik S. I., Gorlova N. I., 2003, *A&A*, 411, 559
- Krejčová T., Budaj J., 2012, *A&A*, 540, A82
- Kurucz R. L., 1992, in Barbuy B., Renzini A., eds, *Proc. IAU Symp. 149, The Stellar Population of Galaxies*. Kluwer, Dordrecht, p. 225
- Kurucz R. L., 1996, in Adelman S. J., Kupta F., Weiss W., eds, *ASP Conf. Ser. Vol. 108, Workshop on Model Atmospheres and Spectrum Synthesis*. Astron. Soc. Pac., San Francisco, p. 2
- Matthews J. M., Kusching R., Guenther D. B., Walker G. A. H., Moffat A. F. J., Rucinski S. M., Sasselov D., Weiss W. W., 2004, *Nat*, 430, 51
- McLaughlin J. A., Hood A. W., de Moortel I., 2011, *Space Sci. Rev.*, 158, 205
- Metcalfe T. S. et al., 2013, *ApJ*, 763, L26
- Morton R. J., Verth G., Jess D. B., Kuridze D., Ruderman M. S., Mathioudakis M., Erdélyi R., 2012, *Nat. Commun.*, 3, 1315
- Musielak Z. E., Rosner R., Stein R. F., Ulmschneider P., 1994, *ApJ*, 423, 474
- Musielak Z. E., Rosner R., Ulmschneider P., 2002, *ApJ*, 573, 418
- Rammacher W., Cuntz M., 2005, *A&A*, 438, 721
- Reiners A., 2012, *Living Rev. Sol. Phys.*, 8, 1
- Rüedi I., Solanki S. K., Mathys G., Saar S. H., 1997, *A&A*, 318, 429
- Saar S. H., 1996, in Strassmeier K. G., Linsky J. L., eds, *IAU Symp. 176, Stellar Surface Structure*. Kluwer, Dordrecht, p. 237
- Santos N. C., Israelian G., Mayor M., 2004, *A&A*, 415, 1153
- Sim S. A., Jordan C., 2005, *MNRAS*, 361, 1102
- Solanki S. K., 1993, *Space Sci. Rev.*, 63, 1
- Solanki S. K., Inhester B., Schüssler M., 2006, *Rep. Prog. Phys.*, 69, 563
- Steffen M., 1993, *Habilitation thesis*, Univ. Kiel
- Stein R. F., Nordlund Å., Georgobiani D., Benson D., Schaffenberger W., 2009a, in Dikpati M., Arentoft T., González Hernández I., Lindsey C., Hill F., eds, *ASP Conf. Ser. Vol. 416, Solar–Stellar Dynamos as Revealed by Helio- and Asteroseismology*. Astron. Soc. Pac., San Francisco, p. 421
- Stein R. F., Georgobiani D., Schaffenberger W., Nordlund Å., Benson D., 2009b, in Stempels E., ed., *AIP Conf. Proc. Vol. 1094, Cool Stars, Stellar Systems, and the Sun 15*. Am. Inst. Phys., Melville, p. 764
- Stello D. et al., 2010, *ApJ*, 713, L182
- Stenflo J. O., 1978, *Rep. Prog. Phys.*, 41, 865
- Taroyan Y., Erdélyi R., 2009, *Space Sci. Rev.*, 149, 229
- Theurer J., 1993, *Diploma thesis*, Univ. Heidelberg
- Ulmschneider P., 1989, *A&A*, 222, 171
- Ulmschneider P., Musielak Z. E., 1998, *A&A*, 338, 311
- Ulmschneider P., Theurer J., Musielak Z. E., 1996, *A&A*, 315, 212
- Ulmschneider P., Theurer J., Musielak Z. E., Kurucz R., 1999, *A&A*, 347, 243
- Ulmschneider P., Fawzy D., Musielak Z. E., Stępień K., 2001a, *ApJ*, 559, L167
- Ulmschneider P., Musielak Z. E., Fawzy D. E., 2001b, *A&A*, 374, 662
- Valenti J. A., Marcy G. F., Basri G., 1995, *ApJ*, 439, 939
- Vieytes M. C., Mauas P. J. D., Diaz R. F., 2009, *MNRAS*, 398, 1495
- Wedemeyer-Böhm S., Scullion E., Steiner O., Rouppe van der Voort L., de La Cruz Rodríguez J., Fedun V., Erdélyi R., 2012, *Nat*, 486, 505

This paper has been typeset from a  $\text{\TeX}/\text{\LaTeX}$  file prepared by the author.